

## REVIEW ON MATERIALS PROPERTIES OF Sn(S,Se) COMPOUND SEMICONDUCTORS USEFUL FOR PHOTOELECTROCHEMICAL SOLAR CELLS

B SUBRAMANIAN, C SANJEEVIRAJA\* AND M JAYACHANDRAN

*Central Electrochemical Research Institute, Karaikudi 630 006, INDIA*

*\* Department of Physics, Alagappa University, Karaikudi 630 003. INDIA*

[Received: 27 March 2002

Accepted: 10 April 2002]

*Thin film semiconducting metal chalcogenides have tailorable properties to use them as storage electrodes in the rechargeable photoelectrochemical solar energy storage cells. Amongst IV-VI semiconducting compounds, tin chalcogenides exhibit an orthorhombic structure with eight atoms per unit cell forming double layer planes normal to the longest axis. The material properties of the layered semiconductors tin selenide (SnSe), tin sulfide (SnS) and tin sulfoselenide (SnSSe) prepared by different methods are presented in this review.*

*Keywords: Semiconductor, chalcogenide, thin film, tin selenide, tin sulfide, tin sulfoselenide*

### INTRODUCTION

In the twenty-first century human society will rely on nuclear power, solar power, ocean thermal energy, tidal power, wind energy and geothermal energy, in addition to the limited amount of energy which can be derived from hydro power and fossil fuels which are getting rapidly depleted. Almost all countries have initiated programmes to develop indigenous alternate energy resources that could solve the crisis. The main objectives of all technological developments are to develop energy sources which may be long lasting, pollution free, easily available and cost effective [1-9]. The review [2] shows that the solar energy and energy conversion are the most preferred energy photovoltaic cells. Single crystal silicon solar cells have been widely employed on space craft. For application in photovoltaic and PEC solar cells, semiconductor thin films like CdSe, CdS, CdHgTe, GaAs, CuInSe<sub>2</sub>, CuInS, CdTe, MoSe<sub>2</sub>, WSe<sub>2</sub>, SrTiO<sub>3</sub>, SnO<sub>2</sub>, In<sub>2</sub>O<sub>3</sub>, TiO<sub>2</sub> have been studied elaborately [7,14]. Recently interest has been shown in using SnSe and SnS as photoelectrodes, in the construction of PEC cells [10,11]. Also tin chalcogenides have attracted attention due to their unmatched applications in producing infrared rays and detection [12,13].

### Methods of thin film deposition

There are several methods for preparing thin films. Some of them are vacuum evaporation, sputtering hot wall epitaxy, spray pyrolysis, chemical vapour deposition, solution growth, electrodeposition, electroless deposition, brush plating, screen printing etc. Discussion about the various methods of film preparation is given by Chopra [14], Maissel and Glang [15] and Behrndt [16]. Chemical deposition techniques like electrodeposition, chemical vapour deposition, brush plating are particularly attractive for large area devices and which are relatively cheap. A simple and brief discussion about the various methods of film preparation is given here.

### Vacuum evaporation

Vacuum evaporation is one of the most widely used deposition techniques. The first evaporated thin films were obtained by Faraday in 1857 when he exploded metal wires in an inert atmosphere. The deposition of a thin film by vacuum evaporation consists of three steps:

- i) Transition of a condensed phase, which may be a solid or liquid into gaseous state
- ii) Vapour traversing the space between the evaporation source and the substrate at reduced gas pressure.



- iii) Condensation of vapor upon arrival on the substrates.

The important control parameters are evaporation rate, substrate temperature and oxygen partial pressure. Several metallic films, semiconductor oxide films and compound semiconducting films have been prepared by various workers [17-19]. Films of well defined composition of multicomponent II-IV, IV-VI and III-V compound semiconducting films are prepared [19].

In the case of resistive heating method, the material is heated in a resistively heated support made up of refractory metals. The simple resistive heating has the limitation of input power. Hence it is very difficult for the high melting point materials to evaporate. Electron bombardment heating is an efficient method to overcome this difficulty.

In principle, this technique is useful to evaporate material with a wide range of evaporation rates. RF heating [20], Laser evaporation [21], exploding wire technique [22], arc evaporation [23] and flash evaporation [24] are the other techniques to prepare thin films by evaporation methods.

#### Hot wall epitaxy

Hot wall epitaxy [25,26] is a vacuum deposition technique whose main feature is the growth of epitaxial layers or thin films under conditions as near as possible to thermodynamic equilibrium with the least loss of material. The main feature of the hot wall epitaxy is the heating of the walls of the chamber which serves the purpose of enclosing and directing the vapour from the source onto the substrate by reducing markedly the deposition of the vapour atoms onto the walls of the chamber. This leads to the following advantages:

- i) Loss of material is avoided
- ii) High vapour pressures of the compound or its different components can be maintained
- iii) The difference between the substrate temperature and the source temperature can be reduced to a minimum value.

#### Sputtering techniques

The process of ejection of atoms by energetic, bombarding ions as a result of momentum transfer from them to the atoms on the surface of a target

material is termed as Sputtering [27,28]. The sputtered atoms, which travel with high velocities in all directions from the target can be collected on any substrate surface held in their paths to form a sputtered thin film. The number of sputtered atom is proportional to the number of ions and hence the sputtering provides a very simple and precise control on the rate of film deposition. Dupuy and Cachand [29] have written useful reviews on sputtering techniques. Both reactive and non-reactive forms of d-c and rf sputtering and recently magnetron and ion beam sputtering have been utilized to deposit various semiconducting films [30].

#### Chemical vapour deposition (CVD)

Chemical vapour deposition techniques have been quite successfully used to prepare epitaxial layers of elemental semiconductors Si and Ge and also the compound semiconductors such as GaAs, GaP, various chalcogenides etc. [31,32]. This method has found wide acceptance because of its simplicity, good reproducibility and easy adaptability to the derived needs. CVD is a technique in which a compound or compounds from the gas phase condense on a substrate surface where a chemical reaction occurs which leads to the production of a solid thin film deposit. The gas composition, flow rate and substrate temperature are the important parameters. Typical deposition rates are 100 - 300 nm/min. The substrate temperature ( $T_{\text{sub}}$ ) is generally in the range of 600-850 K and higher  $T_{\text{sub}}$  paves way for better crystallinity [32].

#### Spray pyrolysis

Chemical spray deposition (CSD) or reactive pulverization or more popularly known as spray pyrolysis. This is a simple technique to prepare thin films. The technique consists of spraying usually an aqueous solution containing soluble salts in appropriate ratios of the constituent atom onto a heated substrate, where the complex undergoes pyrolytic (endothermic) decomposition. The other by-products and the excess solvents escape in the vapour phase. The heated substrate provides the energy for thermal decomposition and subsequent recombination of the constituent species followed by sintering and recrystallization of the clusters of crystals giving rise to adherent and coherent films.



The deposition parameters are solution and carrier gas flow rate, substrate to nozzle distance, substrate temperature and solution composition. This technique is capable of giving high deposition rates 100-500 nm/min and has been an attractive technique for large scale deposition of large area coatings. An ultrasonic atomizing system has been used to narrow down the distribution of droplet size for better surface uniformity [33].

### Solution growth process

The solution growth process was pioneered by Bode [34], Kitaev *et al.* [35] and Chopra [36]. The process itself was first used in 1946 to prepare PbS films for infrared applications. This method is well known for the preparation of chalcogenide films.

The substrates are immersed vertically in the reaction bath and is stirred continuously. The temperature of the bath may be maintained constant. When the ionic product of the metal and hydrogen ion exceed the solubility product of the corresponding chalcogenide, a metal chalcogenide film is formed on the substrate by an ion by ion condensation. Suitably complexing agents should be added in order to eliminate spontaneous precipitation of solutions. Kainthla *et al.* [37] have generated  $\text{Se}^{2+}$  ions by dissolving inorganic sodium seleno sulphate in an alkaline solution.

It is also possible to form multicomponent chalcogenide films over a wide composition range. A variety of variable composition ternary alloys like  $\text{Pb}_{1-x}\text{Mg}_x\text{S}$ ,  $\text{CdSe}_{1-x}\text{S}_x$  has been prepared.

### Electrodeposition

Chandra *et al.* [38-40] investigated the formation and properties of the films of  $\text{MX}_2$  ( $\text{MoSe}_2$  and  $\text{WSe}_2$ ) electrodeposited from the ammonical solutions of  $\text{H}_2\text{MoO}_4 + \text{SeO}_2$  and  $\text{H}_2\text{WO}_4 + \text{SeO}_2$ . An 'induced co-deposition' mechanism has been suggested for the electrodeposition of Mo with Se from aqueous solutions. Electrodeposition of amorphous and polycrystalline  $\text{Sn}_{1+x}\text{Se}$  thin film was reported by Engelken *et al.* [10]. Aqueous ( $\text{SnCl}_2 + \text{H}_2\text{SeO}_3$ ) and non-aqueous ( $\text{SnCl}_2$  and Se dissolved in dimethyl formamide (DMF) electrolytes were used to electrodeposit photoactive semiconducting films of SnSe, which were non stoichiometric. Several IV-VI compound

semiconducting films have been synthesized using electrodeposition.

### Brush plating

Brush plating [41,42] is an electroplating process that is performed with a hand held plating tool rather than using a tank of solution. Brush plating systems vary in degree of sophistication and capabilities. The schematic of brush plating system is given in Fig. 1 [43]. The sophisticated systems use power packs up to 500 A output and have the capacity for producing excellent quality deposits up to 0.25 inch thick on large areas. Brush plated metal coatings are widely used on air-craft for the corrosion protection of steel parts [44]. Brush plated rhodium and gold deposits on copper slip rings are used in submarines and gold plated antenna [42] in the "Voyager" spacecraft.

### Literature survey on SnSe, SnS and SnSe thin films

#### Review on tin selenide (SnSe)

Amongst IV-VI semiconducting compounds, tin chalcogenides exhibit an orthorhombic structure with eight atoms per unit cell [44-46] forming double layer planes normal to the longest axis. SnS and SnSe are isomorphous and crystallize in a rhombic, pseudotetragonal layer structure [47,48]. IV-VI group compound semiconductors have attracted attention due to their unmatched applications in producing infrared rays and detection [26]. SnSe films have great potentialities in holographic recording, memory switching devices and solar cell applications [49-52]. The indirect character of the bandgap of SnSe ( $\sim 0.9$  eV) is a common property of orthorhombic IV-VI compounds [53,54] and has been confirmed by band structure calculations for SnSe [55,56]. Singh and Bedi [57] reported the electrical properties of tin selenide films by flash evaporation onto glass, mica and KCl substrates. Bennouna *et al.* [58] studied fundamental transport and spectral properties of tin compounds in their polycrystalline form. The electronic structure of evaporated films of SnSe is close to the crystalline nature which allows the possibility of using this compound in its polycrystalline form for electronic applications. Nuriev and Sharifova [59] prepared SnSe films by evaporation on NaCl and KCl chips. They have reported that the



structure of SnSe films is influenced by the structure of the substrate, the temperature of the substrate and the stoichiometry of the initial source. X-ray photoemission studies of valence band of SnSe were performed by Shalvoy *et al.* [60] and IR and Raman spectra were analyzed by Chandrashekar *et al.* [61]. Absorption spectra of SnSe have been reported by Guseinova *et al.* [62], Elkorashi [63] and Gang *et al.* [64].

Sharon *et al.* [52,65] have constructed PEC cells using p-SnSe electrodes prepared by the vapour transport method in which the elements in 1:1 proportion react under  $H_2$  atmosphere. Subba Rao and Chaudhuri [66] have studied hall coefficient, photoconductivity and photorelaxation measurements on vacuum-evaporated SnSe films in the temperature range 300-130 K to probe into the mechanism of photoconduction in these films. Bhatt *et al.* [67] have developed p-SnSe/n-SnSe<sub>2</sub> heterojunction solar cells using vacuum evaporation technique employing SnSe and SnSe<sub>2</sub> charges. Freik *et al.* [68] have studied the conductivity type, the carrier density and mobility and the parameters of the real structure of PbTe and SnSe films as functions of the composition and deposition temperature. Engelken *et al.* [10] have deposited SnSe films by electrodeposition and analysed their optical properties and photoconductance. The surface morphology of the electrodeposited SnSe films showed uniform grain size without pin holes [112]. The photoactivity of electrodeposited SnSe films has been studied by Jodgudri and Lokhande [69]. Pramanik and Bhattacharya [70] have also exploited a chemical method for deposition of SnSe thin films. Electrical properties and optical absorption of the evaporated films [71] and the films obtained by solid state reactions have been reported by Quan [72]. Suguna *et al.* [73] have reported the structure, composition, dielectric and A.C. conduction studies on thermal evaporated SnSe films. The materials properties of SnSe is given in Table I.

### Review on SnS

Another interesting member of the IV-VI family of semiconducting compound is SnS. It has great potential in solar energy conversion as well as in optoelectronic devices. The usage of SnS in

photovoltaic cells may be of greater interest, since its optical bandgap of 1.08 eV is similar to that of silicon. The phase diagram of Sn-S system has been characterized by the presence of two compounds, namely SnS and SnS<sub>2</sub> [74] and the two intermediate phases Sn<sub>3</sub>S<sub>4</sub> and Sn<sub>2</sub>S<sub>3</sub> are reported to be peritectic reactions. Unlike SnS<sub>2</sub> counterpart which is n-type, SnS is formed as usually p-type and contains doubly-ionized tin vacancies [74]. Thin films of SnS were chemically deposited on different substrates [75,76]. Nair and Nair [77] have reported the chemical bath deposition of Cu<sub>x</sub>S and SnS thin films on glass substrates and illustrated their applications in solar control coatings. The films showed a photocurrent to dark current ratio of 5-10 under 500 Wm<sup>-2</sup> tungsten halogen illumination [78]. SnS films were deposited [75] on nonconductive substrates by an "electroless" chemical precipitation mechanism using an organic acid/H<sub>2</sub>O bath in which SnCl<sub>2</sub>, S and complexing agents were present. A chemical method was developed for the preparation of tin (II) sulphide thin films on glass substrates at room temperature using Sn<sup>2+</sup> ions complexed with triethanolamine ammonia and thioacetamide as the sulphur source [76]. Electron probe micro analysis and X-ray photoelectron spectroscopy studies were carried out for electrodeposited SnS films by Mishra *et al.* [11]. Electrodeposition was carried out using nonaqueous ethylene glycol bath containing anhydrous SnCl<sub>2</sub> and elemental sulphur. Crystalline SnS is usually a p-type semiconductor, with optical and thermal energy bandgaps of 1.08 eV and 1.20 eV respectively [79,80]. Annealing of chemically deposited SnS films at 558 K in air changed the type of conductivity

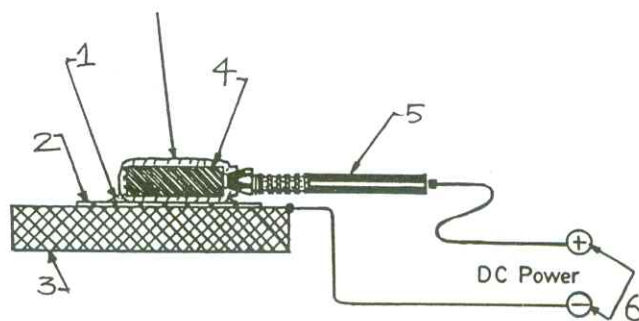


Fig. 1: Schematic diagram of brush plating  
(1) Build-up solution (2) Deposit (3) Substrate  
(4) Anode (5) Stylus Handle (6) Leads

from p- to n-type [81]. Annealing for 24h changed the composition of SnS to SnS<sub>2</sub>. Oxidation at higher temperatures (573-673 K) in open air, changed the sulphide film into oxide film (SnO<sub>2</sub>) [82]. The surface smoothness of the electrodeposited SnS was characterized by AFM analysis [124]. Surface chemical composition of the brush plated SnS films were analysed using XPS analysis [43]. The density of valence band states of SnS has been calculated by the tight-binding method [83] and the structure calculation for SnS using empirical pseudopotential method is presented [84]. The detailed report on photoelectrochemistry (PEC) of layered

semiconductors is given by Levy-Clement and Tenne [85]. PEC behaviour of SnS pellet was studied by Sharon *et al.* [86,87]. The photoactivity of the electrodeposited SnS films and their conduction types were evaluated using photoelectrochemical technique [88]. Lokhande [89] synthesized SnS films by chemical deposition from an acidic bath using sodium thiosulphate as a sulphur source and showed photovoltaic activity. The photovoltaic properties of vacuum evaporated SnS films were studied which showed the following out-put characteristics: a short circuit current density of 7 mA.cm<sup>-2</sup>, an open-circuit voltage of 0.12 V, a fill factor of 0.35 and a

TABLE I: Materials properties of SnSe [10,12,52,61,65]

Type	: p-type
Structure	: Orthorhombic with a = 4.46 (nm), b = 4.19, c = 11.57 Polycrystalline
Indirect bandgap (eV)	: 0.907
Carrier concentration cm <sup>-3</sup>	: 3 x 10 <sup>15</sup> -2 x 10 <sup>18</sup>
Refractive index (n)	: n <sub>a</sub> = 4.55 (1.4 eV); n <sub>b</sub> = 4.10 (1.4 eV)
Resistivity (ohm.cm)	: 7.9
Hole mobility (cm <sup>2</sup> V <sup>-1</sup> s <sup>-1</sup> )	: 110-165 (300 K) 7000 (77 K)
Effective mass of hole	: 1.4 m <sub>0</sub> (m <sub>0</sub> - free electron mass)
Dielectric constant (ε)	: ~12.92
Activation energy (eV)	: 0.44
Absorption coefficient	: 2.5 x 10 <sup>4</sup> cm <sup>-1</sup>
Density of SnSe (gm/cm <sup>3</sup> )	: 6.18
Melting point (K)	: 1133 K
Photovoltaic and device properties of SnSe/SnO <sub>2</sub> :F	: E <sub>g</sub> (eV) : 3.70 V <sub>oc</sub> <sup>g</sup> (mV) : 410 J <sub>sc</sub> <sup>oc</sup> (mA/cm <sup>2</sup> ) : 9.2 F.F. <sup>sc</sup> : 0.49 η (%) : 2.3
<b>PEC properties</b>	
Electrolyte system	: Fe <sup>3+</sup> / Fe <sup>2+</sup>
Flat band potential (V vs SCE)	: 0.66
Efficiency	: 0.16
Stability	: Stable



conversion efficiency of 0.29% were obtained under the illumination of  $100 \text{ mW.cm}^{-2}$  [90]. Deraman *et al.* prepared SnS films by evaporation method and studied the electrical conductivity [91]. Wei Guang-Pu *et al.* synthesized the SnS films by RF sputtering method [92]. Using  $\text{H}_2\text{S}$  and  $\text{SnCl}_4$  as source materials, SnS films were prepared by the plasma enhanced chemical vapour deposition technique [93]. Spray pyrolysis technique was used to prepare p- SnS films on glass substrates in the range, 473-698 K and n-CdS/p-SnS solar cell was produced with an efficiency of about 0.5% [94]. The materials properties of SnS is presented in Table II.

### Review on SnSSe

This ternary compound has recently attracted much interest in solar energy conversion because of the bandgap tailoring effected by the incorporation of S in SnSe. Preparation and properties of mixed crystals of  $\text{Sn}_{(1-x)}\text{Se}_x$  have been reported [95]. The two compounds SnS and SnSe form a continuous series of mixed crystals with a minimum melting point of 1128 K at the composition  $\text{SnS}_{0.5}\text{Se}_{0.5}$ . The crystals are all p-type with hole concentration of about  $10^{18} \text{ cm}^{-3}$ . The band edge absorption is found to be allowed indirect transitions. The band gap of SnS and SnSe at 573 K was 1.08 and 0.90 eV respectively. The bandgap of mixed crystals  $\text{SnS}_{(1-x)}\text{Se}_x$  varies linearly with x [95]. The materials properties of  $\text{SnS}_{0.5}\text{Se}_{0.5}$  is presented in Table III. Results on photoelectrochemical (PEC) and corrosion studies of n-type SnSSe compound were reported [96]. SnSSe was stable in acidic medium, but the stability decreased as pH increased. The PEC behaviour of  $\text{SnS}_{1-x}\text{Se}_x$  solid solution was reported [97- 100].

The solid solution  $\text{SnS}_x\text{Se}_{2-x}$  can be prepared over the entire composition range from  $\text{SnS}_2$  to  $\text{SnSe}_2$ . Compounds obtained are layered semiconductor with  $\text{CdI}_2$  type structure. Optical properties of  $\text{SnS}_x\text{Se}_{2-x}$  (where  $0 < x < 2$ ) have been studied [95]. A very satisfying agreement with the experimental optical data is obtained from a priori pseudopotential calculations for  $\text{SnS}_x\text{Se}_{2-x}$  solid solutions [101].

Literature shows very few reports on SnSSe in their thin film form. Thin films of SnSSe were

deposited by flash evaporation on NaCl crystal as well as on glass substrates [102]. TEM examination of the grown film with NaCl substrate revealed improvement in crystallinity with increasing substrate temperature [102]. The increase of activation energy with substrate temperature was linked with the decrease of resistivity.

### Structural properties of $\text{SnS}_x\text{Se}_{1-x}$

Structural properties of the material play a dominant role in the performance of the devices and a knowledge of the influence of various deposition parameters on the structural properties of thin films is essential before the application of these materials in devices [103-108].

The mixed crystals of composition  $\text{SnS}_x\text{Se}_{1-x}$  have the same crystal structure as SnS and SnSe. No super- structure was observed [109]. The unit cell contains eight atoms, placed in position by the scaled co-ordinates  $\pm (u, 1/4, v)$  and  $\pm (1/2 + u, 1/4, 1/2 - v)$  as in Fig. 2a. The atoms are arranged in two adjacent double layers orthogonal to the largest cell dimensions as shown in Fig. 2b. [110,112]. Within either double layer, each atom has three nearest atom lies in the other double layer and provides the bond between double neighbours and two next nearest neighbours. A sixth nearest neighbouring layers. The resulting highly layered structure, typical of all orthorhombic chalcogenide crystals, causes a strong anisotropy of the physical properties of these compounds [112]. Sophisticated characterization techniques have emerged to understand the multifaceted properties of thin films. X-ray diffraction method is one of the best methods for the estimation of the crystallographic parameters. Fig. 3 shows the XRD pattern obtained for the brush plated SnSe film [111].

Singh and Bedi [113] have reported the structural characterization of SnSe thin films grown by hot wall epitaxy technique onto glass substrates. It was observed that the diffraction peak corresponding to (111) orientation was most prominent. The unit cell dimensions of the orthorhombic SnSe lattice was calculated as  $a = 4.444 \text{ \AA}$ ,  $b = 11.496 \text{ \AA}$  and  $c = 4.151 \text{ \AA}$ .

These dimensions correspond to the low-temperature phase orthorhombic structure of SnSe. An appreciable increase in grain size was observed with increase in substrate temperature. Crystallites as large as 4  $\mu\text{m}$  were observed at a substrate temperature of 558 K. The X-ray diffraction diagram of the SnSe films prepared by solid state reactions [72] indicated the presence of (040) peak and its equivalents (020), (060) and

(080). These SnSe films have a strongly preferred orientation along (0k0). Their crystallites are perpendicular to the (040) plane. It was noted that this preferential orientation was different from that for the evaporated SnSe films with (111) plane [14].

Subba Rao *et al.* [114,115] reported the crystallite size and microstrain values for SnSe thin films of thickness 210-240 nm deposited on glass

TABLE II: Materials properties of SnS [12,61,76]

Type	: Usually p-type; S vacancies n-type; Sb doped n-type
Structure	: Orthorhombic with $a = 4.33$ (nm) Hergenbergite $b = 3.98$ Polycrystalline $c = 11.18$ Polycrystalline
Indirect bandgap (eV)	: 1.14
Carrier concentration $\text{cm}^{-3}$	: $5 \times 10^{17}$
Refractive index (n)	: $n = 3.5$
Resistivity (ohm.cm)	: 0.06
Hole mobility ( $\text{cm}^2\text{V}^{-1}\text{s}^{-1}$ )	: 54 (300 K) 2000 (77 K)
Effective mass of hole	: $0.4 m_0$ ( $m_0$ - free electron mass)
Dielectric constant ( $\epsilon$ )	: 14-19
Activation energy (eV)	: 0.28~0.3
Absorption coefficient	: $2 \times 10^4 \text{ cm}^{-1}$
Density of SnS ( $\text{gm/cm}^3$ )	: 5.0
Melting point (K)	: 1154 K
Photovoltaic and device properties of CdS/p-SnS	: $E$ (eV) : 1.45 $V_{\text{oc}}^g$ (mV) : 120 $J_{\text{sc}}^{\text{oc}}$ ( $\text{mA/cm}^2$ ) : 7 F.F. : 0.35 $\eta$ (%) : 0.29 Illumination $\text{mW/cm}^2$ : 100 Diode quality factor (n) : 3.5
<b>PEC properties</b>	
Electrolyte system	: $\text{Fe}^{3+} / \text{Fe}^{2+}$
Flat band potential (V vs SCE)	: 0.46
Efficiency	: 0.63
Stability	: Stable



TABLE III: Materials properties of  $\text{SnS}_{0.5}\text{Se}_{0.5}$  [103]

Type $\text{SnS}_{(1-x)}\text{Se}_x$	: p-type
Structure	: Orthorhombic (No superstructure) Crystallographic axes (a,b,c) vary linearly with 'X'
Energy gap (eV)	: 1.08-0.90 varies linearly with composition X
Concentration of holes ( $\text{cm}^{-3}$ )	: $10^{17}$ - $5 \times 10^{18}$
Mobility of holes for $\text{SnSSe}$	: 19
for $\text{SnS}_{0.7}\text{Se}_{0.3}$ ( $\text{m}^2\text{V}^{-1}\text{S}^{-1}$ )	: 65 (300 K)
Melting point of $\text{SnS}_{0.5}\text{Se}_{0.5}$ (K)	: 1126 K

substrates kept at different high temperatures using the method of variance and Fourier analysis of the X-ray diffraction line profiles. Variability of the interlayer spacing had also been studied. It was observed that with an increase in the deposition temperature there was a gradual increase in the crystallite size, the r.m.s strain and the  $g$  values.

Vincett *et al.* [116] had shown that the optimum substrate temperature at which the growth of the films with large crystallites was approximately equal to one-third of the boiling point of the material. Santhanam *et al.* [117] had observed that the crystallites of large size were obtained when the substrates were kept at the optimum temperature. Nuriev and Sharifova [59] had reported that the structure of SnSe films depends on the structure of the substrate on which films were deposited and the stoichiometry of the initial source. Films on amorphous (celluloid) substrates had an orthorhombic structure, while those on NaCl and KCl chips had a cubic one. It was noted that for SnSe, the congruently subliming compositions were shifted towards tin [118]. This fact means that one can not obtain a film of stoichiometric composition by free evaporation in a vacuum. The films will always contain excess tin. The cubic modification of SnSe was also found by Arilov *et al.* [119] who obtained SnSe films by vacuum condensation on NaCl crystals. Engelken *et al.* [10] have reported the structural data of electrodeposited  $\text{Sn}_{1\pm x}\text{Se}_x$  films. The dominant peak near 303 K ( $\text{Cu-K}\alpha$ ,  $2\theta$ ) was identified as

SnSe (111) plane and the peaks near 316 and 311 K were also identified as SnSe. Many films were amorphous with no X-ray feature. The films were orange, more transparent and thinner after annealing in a vacuum at 573 K. Figs. 4(a) and

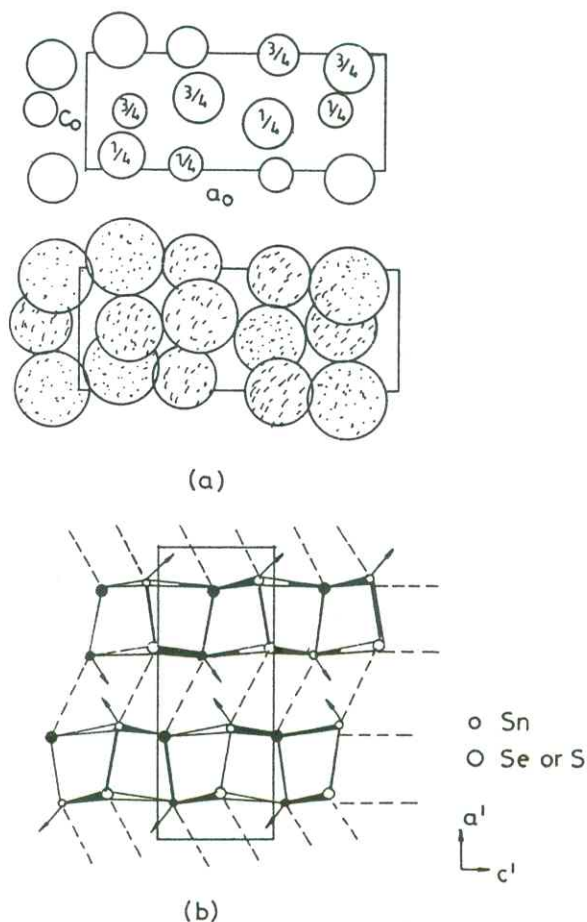


Fig. 2: Crystal structure of  $\text{SnS}_x\text{Se}_{1-x}$  ( $x = 0, 0.5$  and  $1$ )  
(a) arrangement of atoms (b) projection of atoms on  $a$ - $c$  plane



4(b) show the XPS analysis pattern obtained for electrodeposited SnSe films [112].

Pramanik *et al.* [76] had reported the composition of the SnS films prepared by chemical deposition by X-ray diffraction analysis. The films were scrapped off from the substrates and their diffraction profiles were recorded which did not show any sharp peaks, indicating that the films were amorphous. The powder was crystallized by heating at 693 K in an inert atmosphere. The observed XRD peak values were in good agreement with the standard ASTM values confirming the crystalline SnS film formation after annealing. Ristov *et al.* [81] had found that the intensity of the (013) peak increases with increasing pH, showing the increased degree of preferred orientation. It was also noticed that the intensity of diffuse reflection decreases with increasing pH from 3 to 10. Noguchi *et al.* [90] had reported the XRD patterns of vacuum evaporated SnS films on glass substrates at different temperatures. The orientation of SnS films changed from (111) crystal plane to (040) crystal plane with increasing substrate temperature. The (111) crystal plane of the film oriented below 473 K and the (040) crystal plane preferentially oriented above 553 K. A strong peak of (040) crystal plane was noticed in the films deposited on aluminium substrates. The lattice constants of SnS films were found to be  $a = 0.427$  nm;  $b = 1.119$  nm and  $c = 0.398$  nm above 523 K. SnS films exhibited the orthorhombic structure with the distorted NaCl type. The cathodic electrodeposition on ITO/glass and Ti substrates from a solution containing  $\text{SnCl}_2$  and thiosulphate ions were reported by Zainal *et al.* [88]. They observed two strong XRD peaks at  $2\theta = 30.4^\circ$  and  $31.6^\circ$  corresponding to interplanar distances of 2.934 Å and 2.833 Å respectively. These results were in agreement with theoretical values of 2.931 Å for (101) plane and 2.835 Å for (111) of SnS herzenbergite structure. Mishra *et al.* [120] had prepared SnS films by electrodeposition on indium tin oxide - coated glass substrates. The technique was based on a nonaqueous ethylene glycol bath containing anhydrous  $\text{SnCl}_2$  and elemental sulphur. It was observed that there was overlap in some cases with the ITO substrate signals (e.g. the SnS (101) plane at  $2\theta = 30.3^\circ$ ).

Examination of the secondary ITO peak near  $2\theta = 20.1^\circ$ , indicated that the SnS strongly masked the ITO contribution. No phases other than SnS were indicated. SnS thin films were prepared by electrodeposition and brush plating methods from aqueous medium by Subramanian *et al.* [121,124]. The lattice parameter values observed from XRD pattern were  $a = 0.432$  nm,  $b = 1.145$  nm and  $c = 0.399$  nm which compare well with the reported values [120]. The strong XRD peak near  $2\theta = 31.5^\circ$  was indicative of SnS ( $d = 2.83$  Å) for the films prepared by low temperature chemical precipitation were reported by Engelken *et al.* [75,123]. The peak intensities were high and the narrow width indicated large grain sizes. This observation was supported by the larger grain sizes as seen in SEM micrographs [124] shown in Fig. 5. Fig. 6 shows the AFM plot of brush plated SnSe film [111].

As there are only very few reports available on  $\text{Sn}_x\text{Se}_{1-x}$  in the literature to our knowledge, the structural studies of thin film and single crystal SnS<sub>x</sub>Se are presented here. Patel *et al.* [125] prepared thin films of SnS<sub>x</sub>Se by flash evaporation on NaCl crystal as well as on glass substrates. Thin films deposited at 300 K were poor crystalline and fine grained in nature, which is

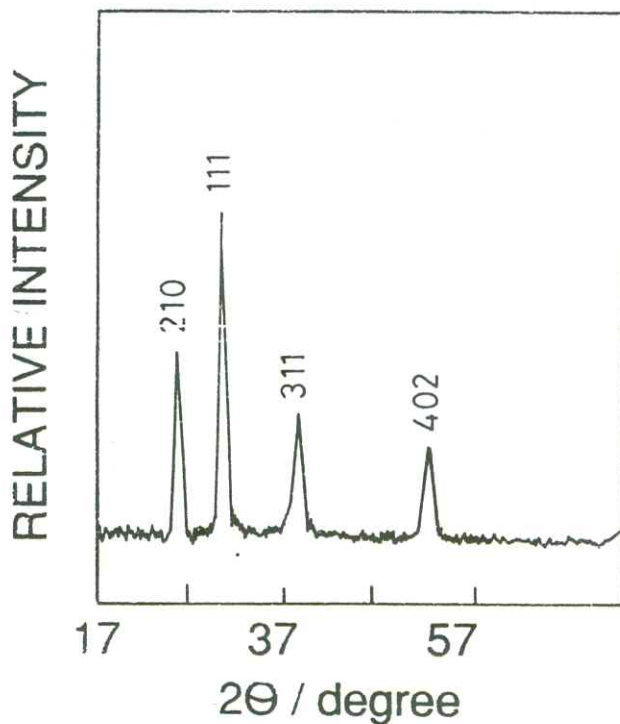


Fig. 3: XRD pattern of the brush plated SnSe thin film



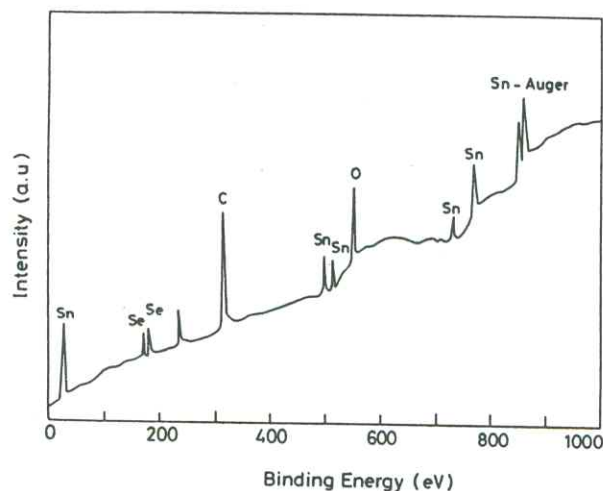


Fig. 4 (a): Survey XPS spectrum for the electrodeposited SnSe film after 2 + 2 minutes argon ion sputtering

attributed to electron beam heating, whereby electron charge or thermal gradient is set up in the poorly conducting film where subjected to the electron beam. Therefore, all the beams were examined under low beam current. The  $d$ -values (interplanar distance) calculated from the electron diffraction pattern were fairly in agreement with the X-ray diffraction data obtained from bulk SnSSe. The electron diffraction patterns revealed that (101) plane is a highly preferred orientation. It was also observed that SnSSe films thus grown are single phase polycrystalline in nature. At higher substrate temperature (630 K) the films were non-stoichiometric because they appeared to possess mixed phases.

X-ray analyses (Debye-Scherrer) showed that the mixed crystal of composition  $\text{SnS}_{(1-x)}\text{Se}_x$  has the same crystal structure as SnS and SnSe. No

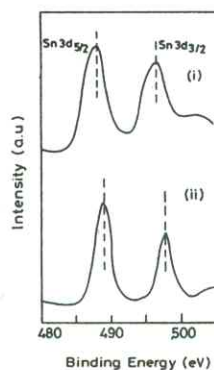


Fig. 4b: High resolution scan of Sn 3d 3/2 and Sn 3d 5/2 (i) unetched top surface (ii) sputtered inner surface

superstructure was observed. The mutual substitution of S and Se atoms occurs at random.

### Optical properties of $\text{SnS}_x\text{Se}_{1-x}$ films

Engelken *et al.* [10] have reported the optical behaviour of electrodeposited SnSe thin films. A moderately strong absorption edge was observed at wavelengths less than 1000 nm. The plot of  $[\text{h}\nu (\text{A}-\text{A}_0)]^{0.5}$  vs  $\text{h}\nu$ , was reasonably linear and when extrapolated to zero absorbance, yielded a bandgap values between 0.85 and 0.95 eV. Plots of  $[\text{h}\nu (\text{A}-\text{A}_0)]^2$  vs  $\text{h}\nu$ , corresponding to direct transitions, showed no constant pattern and unreasonably high bandgap values. Fig. 7 shows the indirect nature of the brush plated SnSe films [111].

Mitchell [126] reported that SnSe single crystals grown by chemical vapour deposition were always p-type and exhibited optical absorbance "cut off energies" of 0.90 and 0.86 eV, corresponding to two different polarizations. A direct transition was observed at 1.2 eV. The spectrum of the annealed film had been shifted toward shorter wavelengths and exhibited a smaller sub-bandgap absorbance. A bandgap,  $E_g \approx 0.95$  eV before annealing and  $E_g \approx 1.30$  eV after annealing was observed. Dang Tran Quan [72] examined the intrinsic absorption edge of the SnSe film synthesized by solid state reaction at 300 K in terms of a direct transition using the equation of Bardeen *et al.* [127]. A bandgap of  $1.195 \pm 0.005$  eV was estimated and it was found to be in the same order as the energy gap (1.210 eV) of evaporated SnSe films [14]. Bhatt *et al.* [105] have calculated the

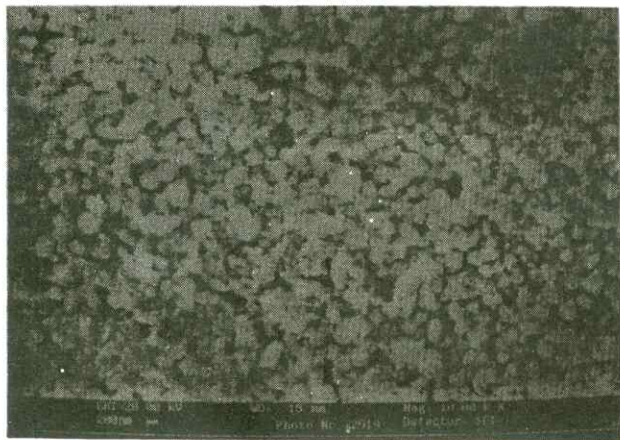


Fig. 5: A typical scanning electron micrograph of a thin film p-SnS



absorption coefficient ( $\alpha$ ) and it had been plotted as a function of radiation energy  $h\nu$ .  $\alpha$  decreased up to  $3.07 \times 10^3 \text{ cm}^{-1}$  at 1.01 eV and then increased to about  $2.5 \times 10^4 \text{ cm}^{-1}$ . This was attributed to the varying surface condition of the films [128]. The ionization energy  $E_i$  of the impurity was found out from the graph and was equal to 0.15 eV. The variation of optical bandgap with thickness of the film was found to be decreased with increasing thickness. The variation was explained in terms of quantum size effect.

A pronounced absorption edge was evident in the vicinity of 700- 800 nm for all the electrodeposited SnS samples synthesized by electrodeposition [120]. The indirect nature of optical transition in SnS was reconfirmed [75]. The  $E_g$  values were obtained in the range 1.35-1.43 eV. A bandgap of about 1.51 eV was observed for a chemically deposited tin (II) sulphide thin films by Pramanik *et al.* [76]. Zainal *et al.* [88] have obtained  $E_g$  value of 0.9 to 1.1 eV for electrodeposited SnS thin films. Vacuum evaporated SnS films have yielded an  $E_g$  value of 1.48 eV [90]. This is larger than the published values and is attributed to the presence of  $\text{Sn}_2\text{S}_3$  (1.9 eV) and  $\text{SnS}_2$  (2.3 eV), though their diffraction peaks were not confirmed by X-ray diffraction. The absorption coefficient near the fundamental absorption edge was larger than  $2 \times 10^4 \text{ cm}^{-1}$  [90]. Ristov *et al.* [81] found that it was possible to vary the optical bandgap

from 2.04 eV to 1.08 eV by changing the degree of crystallinity. The optical absorption edge [129-131], unpolarized infrared transmission [132] and reflectivity [132,133] spectra of SnS had been reported. It is believed that the energy band structure calculations may add to the understanding of the basic processes involved in the absorption of electromagnetic radiations by a semiconductor and subsequent carrier generation [134,135]. The transmission of single crystals of  $\text{SnS}_{(1-x)}\text{Se}_x$  was measured at 573 K and 350 K. The square root of the absorption coefficient in this region was found to be a linear function of photon energy which indicated that the absorption was due to indirect transition of electrons from the valence band to conduction band [136].

Optical absorption of flash evaporated SnSSe thin films were obtained in the wavelength range 200 nm to 1500 nm at room temperature [102]. It was noted that the bandgap energy increased with increased substrate temperature and at higher temperature the value approaches 1.53 eV for the bulk material. It was observed that the increase in the substrate temperature led to an improvement in crystallinity of the films.

#### Electrical properties of $\text{SnS}_x\text{Se}_{1-x}$ films

The electrical properties of SnSe films deposited by flash evaporation onto glass, mica and KCl substrates are reported [57]. The films deposited on KCl substrates showed a lower resistivity than

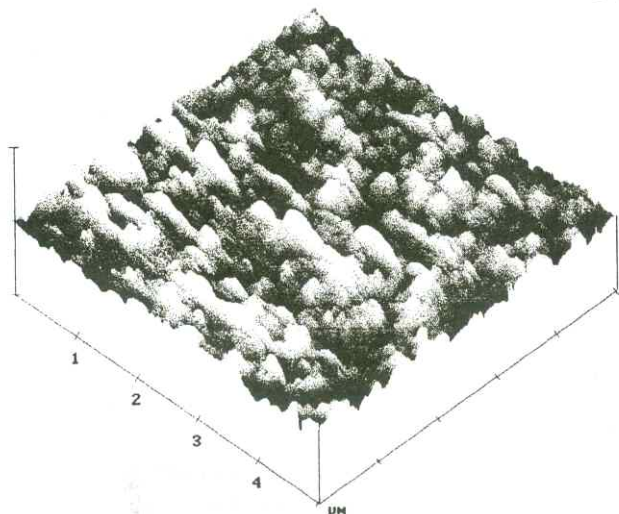


Fig. 6: AFM surface plot of brush plated SnSe film  
Monoscope: AFM Scan size: 5.000  $\mu\text{m}$   
Setpoint: 0 V Scan rate 10.17 Hz No of samples: 256  
X 1.000  $\mu\text{m/div}$  Z 500.000 nm/div

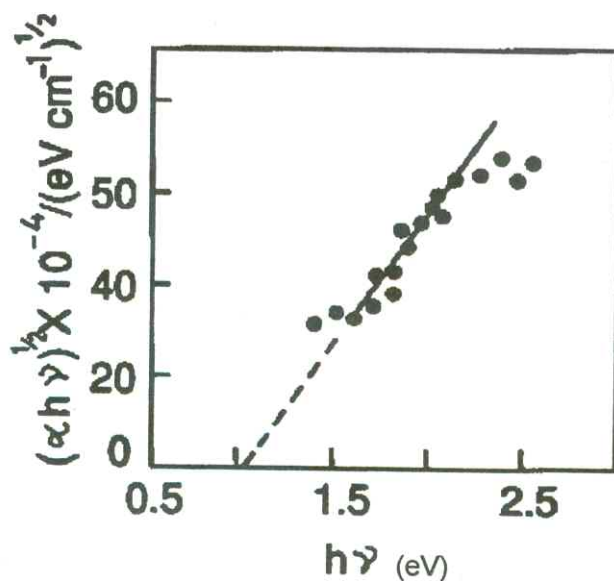


Fig. 7: A plot between  $(\alpha h\nu)^{1/2}$  and  $h\nu$  for SnSe thin film



those deposited on glass and mica substrates. The films were found to be p-type in nature. Hall mobility and carrier concentration were observed to increase with increasing temperature. At room temperature, the resistivity, the Hall mobility and the carrier concentration were found to be 80 ohm cm, 59 cm<sup>2</sup> V<sup>-1</sup> s<sup>-1</sup> and 9.5 × 10<sup>16</sup> cm<sup>-3</sup> respectively. Thermally stimulated currents (TSC) were measured in the structures containing a monocrystalline SnSe film grown by the Hot Wall Epitaxy (HWE) technique. The result showed a total trap density of the order of 10<sup>18</sup>-10<sup>19</sup> cm<sup>-3</sup>. It was observed that trap density increases with decrease in film thickness [137]. Amorphous SnSe films which possess ovonic type switching properties are fabricated using vacuum deposition techniques [138]. Conductivity, photoconductivity and Hall measurements had been carried out on vacuum evaporated, air heated SnSe films of different thickness in the temperature range 300 K-85 K to probe into the mechanism of photoconduction in these films [139]. The average value of the barrier height is found to be in the order of 0.18 eV. The magnitude of the grain boundary potential barrier for different thickness of the film was also estimated from the variation

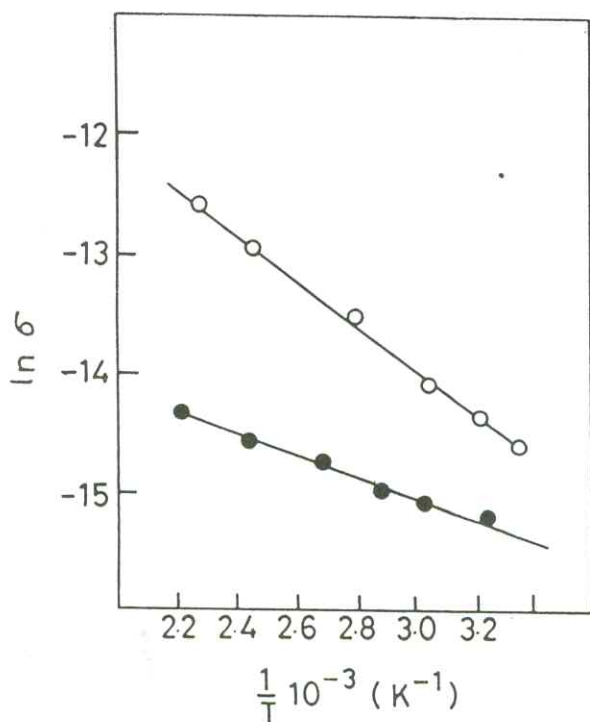


Fig. 8: Conductivity ( $\ln \sigma$ ) vs  $T^{-1}$  (10<sup>3</sup>) for (a) as deposited (b) annealed SnS film

of mobility with temperature and the average value obtained is of the order of 0.17 eV.

The structure, electronic and optical properties of SnSe films prepared by flash evaporation and hot wall epitaxy techniques onto different substrates have been presented [26]. It was observed that the electrical conductivity and carrier mobility of HWE grown SnSe films are comparatively higher than those obtained by conventional evaporation techniques. Observations revealed that the mobility and carrier concentration showed an increase with increasing in thickness [26]. I-V curves obtained for electrodeposited SnSe films [75] were slightly non-linear with a positive  $d^2I/dV^2$  but symmetrical. Hot probe measurements indicated that the films were weakly p-type, consistent with Mitchell's results [126]. The  $\ln$  (conductance)- 1000/T plot exhibits two linear regions with an activation energy of 0.44 eV for the high temperature region and 0.51 eV for the low temperature region.

A method is described, by which the SnS films can be deposited on a glass surface, from aqueous solutions of SnCl<sub>2</sub> and Na<sub>2</sub>S or (NH<sub>4</sub>)<sub>2</sub>S [81]. The conductivity of non-annealed SnS films measured at 293 K and under day light illumination was found to depend on the alkalinity of the SnCl<sub>2</sub> solution. The increase of pH from 3 to 12 led to an increase in conductivity by four orders of magnitude. The films prepared at pH = 3, 10 and 12 with a thickness of 0.1 μm had conductivities of 1 × 10<sup>-7</sup>, 5 × 10<sup>-5</sup> and 6 × 10<sup>-3</sup> Ω<sup>-1</sup>cm<sup>-1</sup> respectively. The  $\ln$  (resistance) vs 1/T yielded the activation energies of 0.3 eV in the high temperature range and 1.1 eV in the low temperature region. Short-time annealing (for 30 min) at 558 K in open air changed the type of conductivity from p-type to n-type. The donor activation energy  $E_d$  = 0.1 eV was determined [81]. Fig. 8 shows the conductivity vs temperature for the electrodeposited SnS films [124]. The electrical characterization of SnS films synthesized by a chemical method on glass substrates at room temperature (300 K) using an Sn<sup>2+</sup> salt solution, triethanolamine, ammonia and thioacetamide as the reagents was studied. The films were found to be amorphous and n type with an optical energy gap of 2.42 × 10<sup>-19</sup> J (1.51 eV) [76]. The



current voltage characteristics of the SnS film with silver contacts were found to be linear, suggesting that silver paint forms an ohmic contact to SnS films.

The electrical properties of SnS films prepared by vacuum evaporation method were reported [96]. Vacuum-deposited SnS films exhibit always p-type conduction with a resistivity of  $13\text{--}20\ \Omega^{-1}\text{cm}^{-1}$ , a carrier density of  $6.3 \times 10^{14}\text{--}1.2 \times 10^{15}\ \text{cm}^{-3}$  and a Hall mobility of  $400\text{--}500\ \text{cm}^2\text{V}^{-1}\text{S}^{-1}$ . The activation energy for conduction was about  $0.28\text{--}0.34\ \text{eV}$ , suggesting the presence of deep acceptor levels, in accordance with the results in the literature [75]. Plots of  $\ln(\text{conductance})$  vs  $T^{-1}$  for the grey-black  $\text{Sn}_{1-x}\text{S}$  ( $E_g \sim 1.0\text{--}1.3\ \text{eV}$ ) synthesized by the CVD technique [81] indicated activation energies between  $0.43$  and  $0.69\ \text{eV}$ . The  $\text{Sn}_{1-x}\text{S}$  films exhibited moderate photoconductance with apparent recombination times  $\sim 1\ \text{ms}$ . SnS films prepared by electrodeposition technique at room temperature on indium tin oxide coated glass substrates showed p-type nature.

Single crystals of  $\text{SnS}_{0.5}\text{Se}_{0.5}$  were used for Hall voltage and resistivity measurements according to Van der Pauw's method [140]. Good electrical contacts were obtained using silver paint or by welding  $100\ \mu$  gold wires to the samples. All crystals prepared by distillation and zone refining were p-type with a free hole concentration at room temperature between  $10^{17}$  and  $5 \times 10^{18}\ \text{cm}^{-3}$  depending on the heat treatment. For SnSe, similar results were reported. The temperature

dependence of the hole mobility measured on cleavage plates of  $\text{SnS}_{0.5}\text{Se}_{0.5}$  showed that only at high impurity concentrations, the mobility was observed to decrease drastically at low temperatures.

### PEC Studies on $\text{SnS}_x\text{Se}_{1-x}$ films

p-SnSe was prepared from its elements by a vapour transport method. SnSe was found to be chemically and photochemically stable in acidic solutions [141]. It was observed that  $\text{Fe}^{3+}$ ,  $\text{Fe}^{2+}$  ( $0.5\ \text{M}\ \text{H}_2\text{SO}_4$ ) redox electrolyte and a platinum counter electrode are the most suitable for constructing a PEC cell with p-SnSe [52]. Nevertheless, the efficiency of the reduction process of  $\text{Fe}^{3+}$  ions at the illuminated SnSe was studied to improve the overall charge-transfer reaction occurring at the interface of the semiconductor and electrolyte. A PEC cell of the type p-  $\text{SnSe}/\text{Fe}^{3+}$ ,  $\text{Fe}^{2+}$  ( $0.5\ \text{M}\ \text{H}_2\text{SO}_4$ ) / Pt was designed to measure the photocurrent and the photovoltage outputs for the efficiency studies. A 250W tungsten halogen lamp with a water filter was used as the power input ( $I_{\text{input}}$ ,  $12\ \text{mW}\cdot\text{cm}^{-2}$ ). The cyclic voltammetric curves as well as photocurrent vs time plots of p-SnSe electrodes indicated the slow photoresponse of the system. A similar behaviour of the electrode was observed with low mobility n-SnS based PEC cells by Sharon and Basavaswaran [141]. The maximum power efficiency and the fill factor were calculated from the I-V characteristics of the cell and were found to be  $0.16\%$  and  $0.19$  respectively. The low efficiency of the cell was attributed to the low carrier concentration. Fig. 9 shows the power output characteristics of p-SnS/ $\text{Fe}^{3+}$ ,  $\text{Fe}^{2+}$ /Pt PEC cell [142].

The cyclic voltammetric curves in a  $0.1\ \text{M}\ \text{Fe}^{3+}$ ,  $\text{Fe}^{2+}$  redox system with platinum, as well as in dark and illuminated conditions of p-SnSe electrodes showed that the cathodic current was found to be light intensity dependent, as expected for a p-type semiconductor. However, an anodic current was observed in the dark as well as under illuminated conditions (beyond the potential of  $+0.5\text{V}$ ). The small anodic current could be due to either the photo-oxidation of anion impurities present in the redox couple or a strong absorption of ions on the electrode surface [142,143]. The

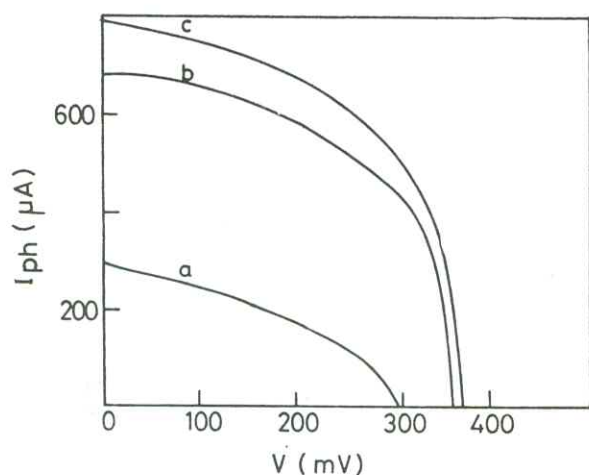


Fig. 9: The power output characteristics of p-SnS/ $\text{Fe}^{3+}$ ,  $\text{Fe}^{2+}$ /Pt PEC cell



photocurrent method was used to determine the bandgap of the semiconductor. The photocurrent was measured from 200 nm to 950 nm [144]. The value of 1.04 eV recorded was close to the values obtained from reflectance (0.9 eV) and conductivity (0.85 eV) methods [141]. The flat-band potential, using the Mott-Schottky relation [145,146] was determined for the system p-SnSe/Fe<sup>3+</sup>, Fe<sup>2+</sup>/Pt and found to be 0.66 V (SCE). The acceptor concentration  $N_A$  was calculated as  $1.55 \times 10^{18} \text{ cm}^{-3}$ . This value differed from the value of  $5.55 \times 10^{16} \text{ cm}^{-3}$  obtained from Hall effect studies. The width of the space charge layer was calculated to be  $2.425 \times 10^{-5} \text{ cm}$ . Fig. 10 shows Mott - Schottky plot for a p-SnSe/Fe<sup>3+</sup>, Fe<sup>2+</sup>/Pt system [111].

SnSe films were electrodeposited onto stainless steel substrates and the photoconductivity was studied by constructing a PEC cell using Fe<sup>3+</sup>/Fe<sup>2+</sup> electrolyte [69]. The films showed p-type semiconducting nature. Flat band potential of the constructed PEC cell was 0.7 V (SCE). The current-voltage (I-V) characteristics were obtained in dark and under illumination (80 mW.cm<sup>-2</sup>). The estimated energy conversion efficiency and the fill factor were 0.0104 % and 0.54 % respectively. The low efficiency was attributed to the presence of surface states and grain boundaries which can act as recombination centres for the photogenerated

carriers [147,148]. The value of the junction ideality factor (A) calculated from the graph of log(I) vs V was found to be 4.0.

A new technique to measure surface conductivity of pellets or thin films was developed [149] which can also provide (i) flat-band potential at a desired pH, (ii) barrier height developed at the interface of semiconductor-electrolyte at any desired pH and (iii) flat-band potential at a desired surface charge present at the semiconductor. A model has been developed to explain the mechanism of surface conductivity of a semiconductor, such as n- $\alpha\text{-Fe}_2\text{O}_3$  or n-SnS or p-SnSe.

The photoactivity of SnS thin films was prepared by room temperature electrodeposition technique on indium tin oxide coated substrates [120]. A well-behaved semiconductor electrode is expected to show rectifying behaviour in the polarization region corresponding to minority carrier current flow [150]. Polarisation curves for the SnS thin film samples in a Fe(CN)<sub>6</sub><sup>3-/4-</sup> redox electrolyte revealed partial rectification for cathodic current flow through the sample in the dark. This incomplete rectification is attributable to defects (eg., grain boundaries) in the (polycrystalline) thin film. Dark measurements quickly established the SnS samples as p-type. PEC measurements were done on SnS in contact with a S<sub>2</sub>O<sub>3</sub><sup>2-</sup> redox electrolyte. The photocurrent onset was observed at ~0.35 V. The shape of the photocurrent spike was discussed [151].

Photoaction spectrum of SnS electrode showed a gradual rise in the photocurrent near the band edge is indicative of an indirect bandgap material. A value for the indirect bandgap of 1.10 eV is obtained. SnSe also characterised by an indirect bandgap in the same energy range.

Dark and photocorrosion behaviour of SnS films was discussed with the aid of Pourbaix diagrams [120]. The stability regions of the various species in the Sn-S-H<sub>2</sub>O system were analysed using Pourbaix diagrams. Thermodynamic data were collected from the literature [152-155]. Thermodynamic analyses suggest the following reactions for the cathodic and anodic corrosion process associated with the dissolution of SnS films.

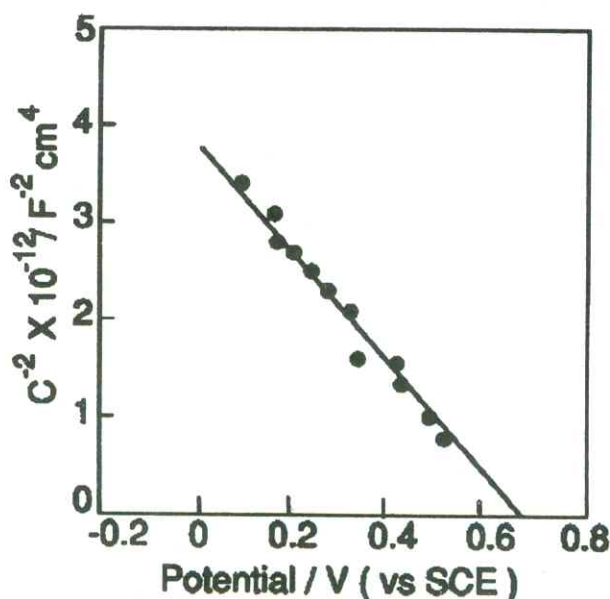
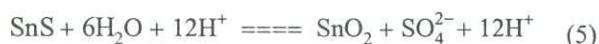
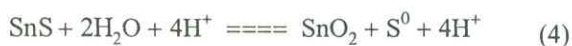
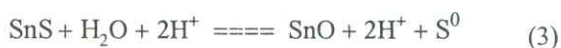
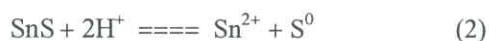
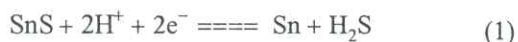


Fig. 10: Mott-Schottky plot for a p-SnSe/Fe<sup>3+</sup>, Fe<sup>2+</sup>/Pt PEC cell





The surface energy levels of SnS, estimated from the flat band potential and the  $E_g$  information, have been superimposed on the Pourbaix diagram. This sort of correlation was employed by [156] for corrosion analyses of other semiconductor electrodes. Since these decomposition potentials lie within the bandgap region, both electrons and holes can corrode SnS [156-158].

SnS films on glass substrates at room temperature prepared by chemical method were found to be photoconducting; hence the spectral response of the photocurrent was ascertained for the determination of bandgap of films. The spectrum had a maximum at 830 nm corresponding to 1.49 eV [76].

The photoactivity measurement of the electrodeposited SnS films on ITO substrate was carried out in contact with  $\text{Fe}^{3+}$  and thiosulphate solution. The light was manually chopped to better delineate the dark and the photocurrent. The latter which was again apparent on the cathodic directions thus confirmed the p-type nature of the deposit [88].

The  $\text{Sn}_{1-x}\text{S}$  films prepared by low temperature chemical precipitation and vapour deposition exhibited moderate photoconductance with apparent recombination times  $\sim 1$  ms [33]. Supporting electrolytes ( $\text{Li}^+$ ,  $\text{Na}^+$ ,  $\text{K}^+$  and  $\text{Cs}^+$ ) are found to suppress the photocorrosion and enhance the fill factor of a PEC cell formed with n-SnS and p-SnSe electrodes [75]. An increase of fill factor has been observed in the order of  $\text{Li}^+ < \text{Na}^+ < \text{K}^+ < \text{Cs}^+$ . It is concluded that the addition of suitable supporting electrolytes, like  $\text{Cs}^+$  ions can help in improving the overall photoconversion

efficiency of a semiconductor electrode in a PEC cell.

PEC properties of solid solutions of SnS-SnSe are reviewed first. The studies on SnSSe films prepared by the both techniques have been carried out to characterise their PEC properties. As there are no reports available in the literature for the PEC properties of  $\text{SnS}_x\text{Se}_{1-x}$  thin films. PEC and corrosion study made on n-type SnSe is presented. Single crystals of n-type  $\text{SnS}_x\text{Se}_{2-x}$  ( $x = 1.04$ ) obtained both by transport and Bridgman methods exhibit an energy gap of 1.53 eV [96]. SnSSe has a diode-like blocking behaviour in acidic solutions (the dark current being equal to  $4 \times 10^{-7} \text{ A.cm}^{-2}$  at anodic potentials); however, the dark current increased with increasing pH and at pH = 14 a substantial increase in anodic current was observed. A sharp increase in current was observed at pH values greater than 7. The anodic current was accompanied by the corrosion of the sample. The corrosion in alkaline solution was enhanced upon addition of the oxidized state of a redox reagent such as  $\text{Fe}(\text{CN})_6^{3-}$ . The dark current and the corrosion intensity increased with increasing concentration of  $\text{Fe}(\text{CN})_6^{3-}$ . The corrosion rate as well as the magnitude of the anodic current depends on pH and the concentration of the oxidizing state of the couple. Light-driven reactions in both acidic and alkaline media are corrosion reactions.

## CONCLUSION

A survey on less expensive less extensively studied tin selenide, tin sulfide and tin sulfoselenide materials. The materials properties of the films prepared by techniques like flash evaporation, hot wall epitaxy, vapour transport method, solid state reaction, electrodeposition and brush plating are reported. The films prepared by most of these methods are polycrystalline and show p-type semiconducting nature. The structural, surface morphology and optical studies reveal that device quality semiconducting tin chalcogenide thin films can be prepared.

## REFERENCES

1. H Tributsch, *Proc Indian Acad Sci (Chem Sci)*, **105** (1993) 315
2. A K Barua, *Ind J Pure and Appl Phys*, **34** (1996) 669



3. Jaspart Singh, *Semiconductor Optoelectronic Devices; Physics and Technology*, McGraw Hill Inc, New York (1995)
4. D Anderson and R H Williams, *United Nations Development Programme*, Technical Paper 6 (World Bank Report, Washington DC 1993)
5. E S Sabisky, *Sol Energy Mater Sol Cells*, **40** (1996) 55
6. D Anderson and C D Bird, *Oxford Bulletin of Economic Statistics*, **54** (1992) 227
7. H J Hovel, *Semiconductors and Semimetals, Vol 11, "Solar Cells"* Academic Press, New York (1975)
8. A L Fahrenbruch and R H Bube, *"Fundamentals of Solar Cells Photovoltaic solar energy conversion"*, Academic Press, New York (1983)
9. K S Chandra Babu, O N Srivatsava and G V Subba Rao, *Current Science*, **66(10)** (1994) 715
10. R D Engelken, A K Berry, T PO Van Doren, J L Boone and A Shanazary, *J Electrochem Soc*, **133** (1985) 581
11. K Mishra, K Rajeshwar, Alex Weiss, M Murley, D Robert Engelken, Mike Slayton and McCloud, *J Electrochem Soc*, **136** (1989) 1915
12. R S Allgaier and W W Scanlon, *Phys Rev*, **111** (1958) 1029
13. D Greig, *Phys Rev*, **120** (1969) 358
14. K L Chopra and S R Das, *Thin film solar cells*, Plenum Press, New York (1983)
15. M Sharon, *Photoelectrochemical Solar Cells*, (Eds) K S V Santhanam and M Sharon, Elsevier, Netherlands (1988)
16. K H B Behrndt, *"Thin Films" American Society of Metals*, New York (1964)
17. E Shanthi, A Banerjee, V Dutta, A Banerjee and K L Chopra, *J Appl Phys*, **53** (1982) 1615
18. P Nath, R F Bunshah, B M Basol and O M Staffsud, *Thin Solid Films*, **72** (1980) 463
19. M V Garcia-Cuenca, M Manchon, M Varela, A Lousa and J L Morenza, *Sol Energy Mater*, **17** (1988) 347
20. E A Roth, E A Margerum and L Jestain, *J Phys Radium*, **20(4)** (1965) 147
21. H M Smith and A F Turner, *Appl Opt*, **4** (1965) 147
22. M Faraday, *Phil Trans Roy Soc, London*, **147** (1857) 145
23. M S P Lucas, H A Owen, Jr W C Stewart and C R Vail, *Rev Sci Instr*, **32** (1961) 203
24. L Haris and B M Seigal, *J Appl Phys*, **19** (1948) 739
25. R W Cahn (Ed), *Materials Science and Technology - A comprehensive treatment, Vol 15, VCH, Weinheim, FRG* (1991)
26. R K Bedi, *Proc Conference on the Physics and Technology of Semiconductor Devices and Integrated Circuits*, (Eds) B S V Gopalam and J Majhi, SPIE, Vol 1523, Tata Mc Graw Hill, New Delhi (1992) 104
27. L Maissel, *Handbook on Thin Film Technology, P 4-1*, (Eds) L I Maissel and R Glang) McGraw Hill Book Co, New York, USA, (1970)
28. J C C Fan, F J Bachner and G H Poley, *Appl Phys Lett*, **31** (1977) 73
29. H S Dupuy and A Cachand, *Physics of non-metallic thin films*, Plenum Press, New York (1976),
30. J Szezyrkowski and A Cyapla, *Thin Solid Films*, **46** (1977) 127
31. S K Ghandi, R Sivilly and J M Borrego, *Appl Phys Lett*, **34** (1979) 833
32. T M Ray Koov, *Thin Solid Films*, **164** (1987) 301
33. E Shanthi, A Banerjee and K L Chopra, *Thin Solid Films*, **88** (1982) 93
34. D E Bode, *Proc Natl Electron Conf*, **19** (1963) 630
35. G A Kitaev, A A Uritskaya and S G Mokrushin, *Russ J Phys Chem*, **39** (1965) 1101
36. K L Chopra, *Thin film phenomena*, McGraw Hill, New York (1969)
37. R C Kainthla, D K Pandya and K L Chopra, *J Electrochem Soc*, **127** (1980) 277
38. S Chandra, O N Srivastava and S N Sahu, *J Phys D, Appl Phys*, **17** (1984) 2115
39. S Chandra, O N Srivastava and S N Sahu, *Phys Stat Sol(a)*, **88** (1985) 497
40. S Chandra, O N Srivastava and S N Sahu, *Phys Stat Sol(a)*, **89** (1985) 321
41. J C Norris, *Met Finish*, **86(7)** (1988) 45
42. J C Norris, *Met Finish*, **86(8)** (1988) 45
43. M Jayachandran, S Mohan, B Subramanian, C Sanjeeviraja and V Ganesan, *J Mat Sci Lett*, **20** (2000) 381-383
44. K R Baldwin and C J E Smith, *Plat and Surf Finish*, July (1997)
45. W Holfmann, *Z Kristalllogr*, **91** (1935) 161
46. A Okazaki and L Veda, *J Phys Soc Jpn*, **11** (1956) 497
47. W Hoffman, *Z Kristalllogr*, **92** (1935) 161
48. A Okazaki, A Okazaki and L Veda, *J Phys Soc Jpn*, **11** (1956) 470
49. J J Loferski, *J Appl Phys*, **27** (1956) 777
50. M Rodot, *Acta Electron*, **18** (1975) 345
51. V P Bhatt, K Gireesan and C F Desai, *Cry Res Tech*, **25** (1990) 209
52. M Sharon, K Basavaswaran and N P Sathe, *J Sci Ind Res*, **44** (1985) 593
53. T Grandke and L Ley, *Phys Rev B*, **16** (1977) 832
54. A W Parke and G P Srivastava, *Phys Stat Sol (b)*, **86** (1978) 871
55. R Car, G Giucci and L Quartapalle, *Phys Stat Sol (b)*, **86** (1978) 871
56. G Gincci, A Guarnieri, G L Masserini and L Quartapalle, *Solid State Commun*, **29** (1979) 75
57. J P Singh and R K Bedi, *Thin Solid Films*, **199** (1991) 9
58. A Bennouna, P Y Tessier, M L Priol, Q Dang Tran and S Robin, *Phys Stat Sol (b)*, **117** (1983) 51
59. I R Nuriev and A K Sharifova, *Sov Phys Crystallogr*, **34(4)** (1989) 635
60. R B Shalvoy, G B Fisher and D J Shiles, *Phys Rev*, **B15** (1977) 2021
61. H R Chandrasekaran, R G Humphrey, U Zwick and M Cardona, *Phys Rev B*, **15** (1977) 2177



62. D A Guseinova, G Z Krivatte and M M Mandov, *Sov Phys Semicond*, **19** (1985) 923
63. A M Elkorashi, *J Phys Chem Solids*, **47** (1986) 497
64. A K Garg, A K Jain and O P Agnihotri, *Ind J Pure and Appl Phys*, **21** (1983) 276
65. M Sharon and K Basavaswaran, *Solar Cells*, **25** (1988) 97
66. T Subba Rao and A K Chaudhuri, *J Phys D Appl Phys*, **19** (1986) 861
67. V P Bhatt, K Gureesan and C F Desai, *Ind J Pure and App Phys*, **29** (1991) 27
68. O M Freik, M F Pavlyuk, A K Shkolnyi, V V Prokopiv, Ya V Ogordnik and M A Lopyanka, *Inorganic Materials*, **26** (1990) 216
69. S A Jodgudri and C D Lokhande, *Bull Electrochem*, **11(10)** (1995) 487
70. P Pramanik and S Bhattacharya, *J Material Sci Lett*, **7** (1988) 1305
71. D T Quan, *Phys Stat Sol (a)*, **86** (1984) 421
72. D T Quan, *Thin Solid Films*, **149** (1987) 197
73. P Suguna, D Mangalraj, S K Narayanadass and P Meena, *Phys Stat Sol (A)*, **15** (1996) 24
74. N Kh Abrikosov, V F Bankina, L V Paretskaya, L E Shelimova and E V Skudnova, in 'Semiconducting IV-VI compounds', A Tybulewicz, Eng 75, Translation, Ed Chapt II, Plenum Press, New York (1969) 65
75. R D Engelken, H E McCloud, C Lee, M Slayton and A Ghoreishi, *J Electrochem Soc*, **134** (1987) 2696
76. P Pramanik, P K Basu and S Biswas, *Thin Solid Films*, **150** (1987) 269
77. P K Nair and M T S Nair, *J Phys D: Appl Phys*, **24** (1991) 83
78. M T S Nair and P K Nair, *Semicond Sci Technol*, **6** (1991) 132
79. W Albers, C Haas, H I Vink and I D Wassher, *J Appl Phys*, **10** (1961) 2220
80. P M Nikolic and D M Todorovic, *J Phys C Solid State Phys*, **20** (1986) 39
81. M Ristov, Gj Sinadinovski, I Groydanov and M Mitreski, *Thin Solid Films*, **173** (1989) 53
82. I Grozdanov, M Ristor, Gj Sinadinovski and M Mitreski, *Fizika*, **21** (1989) 320
83. H Neumann and A Kosakov, *Phys Stat Sol (b)*, **85** (1978) K11
84. A W Parke and G P Srivastava, *Phys Stat Sol (b)*, **101** (1980) K31
85. C Levy-Clement and R Tenne, "Photoelectrochemistry and Photovoltaics of layened semiconductors", (Ed) A Aruchamy, Kluwer Academic Publications, London (1992) pp 155-194
86. M Sharon, P Veluchamy, C Natarajan and Kumar, *Electrochimica Acta*, **36** (1991) 1107
87. M Sharon, "Photoelectrochemical Solar Cells" Vol 50, Elsevier Publications, Oxford (1988) 262
88. Z Zainal, M Z Houssein and A Ghazah, *Sol Energy Mater Sol Cells*, **40** (1996) 347
89. C D Lokhande, *J Phys D: Appl Phys*, **23** (1990) 1703
90. H Noguchi, A Setiyadi, H Tanamura, T Nagatomo and O Omoto, *Sol Energy Mater and Sol Cells*, **35** (1994) 325
91. K Deraman, S Sakran, B B Ismail, Y Wahab and R D Gould, *Int J Electronics*, **76** (1994) 917
92. Wei Guang-Pu, Zhang Zhi-Lin, Zhao Wei-Ming, Gao Xiang-Hong, Chen Wei-Qun, H Tanamura, M Yamaguchi, H Noguehi, T Nagomoto and O Omoto, *IEEE*, **2** (1994) 2402
93. A Ortiz, J C Alonso, M Garcia and J Toriz, *Semicond Sci and Tech*, **11(2)** (1996) 243
94. N Koteswara Reddy and K T Ramakrishna Reddy, *IEEE* (1997) 1451
95. F Huiller, "Structural chemistry of layer type phases, in (Eds) F Ley, D Reifel, Dordrecht-Holland/Boston (1976)
96. B Fotouchi, A Katty and O Gorochov, *J Electrochem Soc*, **132** (1985) 2181
97. R D Engelken and McCloud, *Bull Amer Phys Soc*, **29** (1984) 2806
98. A Katty, B Foutouchi and O Gorochov, *J Electrochem Soc*, **131** (1984) 2806
99. B Foutouchi, A Katti and R Parsons, *J Electroanal Chem*, **183** (1985) 303
100. O H Husser, H Von Kanel and F Levy, *J Electrochem Soc*, **132** (1985) 810
101. F Aymerich, F Meloni and G Mula, *Solid State Communications*, **12** (1973) 139
102. S G Patel, S K Arora, R G Patel and Ajay Agarwal, *Proc on the Physics and Technology of Semiconductor Devices and Integrated Circuits*, (Eds) B S V Gopalam and J Majhi, *SPE*, Vol 1523, Tata Mc- Graw Hill, New Delhi, B S V Gopalam and J Majhi, *SPIE* (1992) 149
103. P A Lee, G Said, R Davis and T H Lim, *J Phys Chem Solids*, **30** (1969) 2719
104. D I Bletskan, I F Kopinets, P P Pogorsh, E N Salkova and D V Chepor, *Kristallografiya*, **20** (1978) 1008
105. V P Bhatt, K Gireesan and C F Desai, *Cryst Res Technol*, **24** (1989) 187
106. M F Ladd and R A Palmer (Eds), *Structure determination by X-ray Crystallography*, Plenum Press, New York (1964) 71
107. H E Bennet and J M Bennet in G Hass and R E Thun (Eds), *Physics of Thin Films Vol 4*, Academic Press, New York (1967)
108. D Bhattacharya, S Chaudhuri, A K Pal and S K Battacharya, *Vacuum*, **42** (1991) 1113
109. W Albers, C Haas, H Ober, G R Schodder and J D Wasscher, *J Phys Chem Solids*, **23** (1962) 215
110. R W G Wycoff, *Crystal Structure*, Wiley, New York (1963)
111. B Subramanian, C Sanjeeviraja and M Jaya chandran, *J Cryst Growth*, **234** (2002) 421-426
112. B Subramanian, T Mahalingam, C Sanjeeviraja, M Jayachandran and Mary Juliana Chockalingam, *Thin Solid Films*, **357** (1999) 119
113. J P Singh and R K Bedi, *J Appl Phys*, **68** (1990) 2776



114. T Subba Rao, B K Samantaray and A K Chaudhuri, *Thin Solid Films*, **165** (1988) 257
115. T Subba Rao, B K Samantaray and A K Chaudhuri, *J Mater Sci Lett*, **4** (1985) 743
116. P S Vincett, W A Barlow and G Roberts, *J Appl Phys*, **48** (1977) 3800
117. S Santhanam, B K Samantaray and A K Chaudhuri, *J Phys*, **15** (1982) 2531
118. N Kh Abrikosov and L E Shelimova, *Semiconducting Materials based on  $A^{IV}B^{VI}$  compounds (in Russian)*, Nauka, Moscow (1975)
119. A S Arilov, R M Imamov and S N Nevasardyan, *Kristallografiya*, **24** (1979) 874
120. K Mishra, K Rajeshwar, A Weiss, M Murley, R D Engelken, M Slayton and H E McCloud, *J Electrochem Soc*, **136** (1989) 1915
121. B Subramanian, T Mahalingam, C Sanjeeviraja, M Jayachandran and Mary Juliana Chockalingam, *Bull Electrochem*, **14** (1998) 398
122. B Subramanian, C Sanjeeviraja, M Jayachandran, S Mohan and Mary Juliana Chockalingam, *Proc SPIE International Symposium on photonics and Applications (ISPA '99) Vol 3896*, (1999) 474
123. R D Engelken and H E McCloud, *Bull Amer Phys Soc*, **29** (1984) 1501
124. B Subramanian, C Sanjeeviraja and M Jayachandran, *J Mat Chem Phys*, **71(1)** (2001) 40-46
125. S G Patel, S K Arora, R G Patel and Ajay Agarwal, *Thin Film Characterization and Applications, Proc of the National Conference*, (Eds) S A K Narayanadass and D Mangalraj (1996)
126. O L Mitchell and H Levinstein, *Bull Amer Phys Soc*, **6** (1959) 161
127. J Bardeen, F J Blatt and L H Hall, R Breekenridge, Russel and T Hahn (Eds), *Photoconductivity Conf*, Wiley, New York (1956)
128. Y G Yu, A S Yue and Jr O M Stafsudd, *J Cryst Growth*, **54** (1981) 247
129. D Wasscher, *J Phys Chem Solids*, **23** (1962) 215
130. W Albers, C Haas, H J Vink and J D Wasscher, *Appl Phys*, **32** (1961) 2220
131. P Ambros, D Geralaes, N A Economon, *Phys Chem Solids*, (1974) 537
132. M Nikolic, S S Vijatovic, O H Hughes, C J Stran and J M Chamberlain, *Proc of the International Conference in Physics of Semiconductors*, (Eds) M H Pilkuh, Tenbner, Stuttgart (1974)
133. C Haas and M M G Corbey, *J Phys Chem Solids*, **20** (1961) 197
134. S Wei and H Krakauer, *Phys Rev Letters*, **55** (1985) 1200
135. X Huoping, L Changlu, W Jianxin, Z Schichang, S Xiaohong, L Zixin, Z Zuyaw and L Zugang, *Sci China Ser E Technol Sci*, **40** (1997) 361
136. S Adachi and T Taguchi, *Phys Rev B*, **43** (1991) 9569
137. J P Singh and R K Bedi, *Jpn J Appl Phys*, **29** (1990) 869
138. C R Baxter and W D Mehennan, *J Vac Sci Technol*, **12** (1975) 110
139. T Subba Rao and A K Chaudhuri, *J Phys D Appl Phys*, **18** (1985) 35
140. W Albers, C Haas, H Ober, G R Schodder and J D Wasscher, *J Phys Chem Solids*, **23** (1962) 215
141. M Sharon and K Basavaswaran, *Sol Cells*, **20** (1987) 323
142. B Subramanian, C Sanjeeviraja and M Jayachandran, *J Mat Sci Lett (communicated)*
143. H R Sprunken, R Schmacher and R N Schindler, *Faraday Discuss Chem Soc*, **70** (1980) 55
144. D E Scaife, *Sol Energy*, **25** (1980) 41
145. N F Mott, *Proc R Soc London Ser A*, **171** (1939) 27
146. W Schottky, *Z Phys*, **113** (1939) 367; **118** (1942) 539
147. J Reichman and M A Russake, in *Photo effects at Semiconductor electrolyte interface* (Eds) A I Nozik, *ACDS SYM*, **146** (1981) 359
148. S W Franka and A J Bard, *J Amer Chem Soc*, **97** (1975) 7472
149. M Sharon, B M Prasad and K Basavaswaran, *Ind J Chem*, **28** (1989) 935
150. H Gerischer, in *"Physical Chemistry*, H Eyring, D Henderson and W Jost, (Eds) Vol IX A, Academic Press, New York (1970)
151. K L Hardee and A J Bard, *J Electrochem Soc*, **124** (1977) 215
152. M Pourbaix, *"Atlas of Electrochemical Equilibria"*, p 476, Pergamon Press, New York (1966)
153. W M Latimer, *"Oxidation Potentials"*, p 243, Prentice-Hall, Englewood Cliffs, New Jersey (1952)
154. R M Smith and A E Martell, *"Critical Stability Constants"*, P 1, Plenum, New York (1976)
155. *Standard Potentials in Aqueous Solution*, A J Bard, R Parsons and J Jordan (Eds), p 189, Marcel Dekker, New York (1985)
156. S M Park and M E Barber, *J Electroanal Chem*, **99** (1979) 67
157. H Gerischer, *J Electroanal Chem*, **82** (1977) 133
158. M Sharon and K Basavaswaran, *Ind Chem*, **28** (1989) 698